

Current Research in **Neuroscience**

ISSN 1996-3408



Academic
Journals Inc.

www.academicjournals.com



Research Article

Activation of Hilar Mossy Cells and Dentate Granule Cells During Sharp Wave/Ripples

¹Ayako Ouchi, ¹Nobuyoshi Matsumoto and ^{1,2}Yuji Ikegaya

¹Laboratory of Chemical Pharmacology, Graduate School of Pharmaceutical Sciences, The University of Tokyo, 7-3-1 Hongo, Bunkyo-ku, 113-0033 Tokyo, Japan

²Center for Information and Neural Networks, National Institute of Information and Communications Technology, Suita, 565-0871 Osaka, Japan

Abstract

Background and Objective: Sharp waves (SWs)/ripples are high-frequency oscillations emitted by the hippocampus mainly during slow-wave sleep or quiet rest states and contribute to offline memory consolidation. They are thought to be initiated in the CA3 subregion and propagate to the downstream regions, including the CA1 area, the subiculum and the entorhinal cortex. At the same time, they also propagate from the CA3 subregion back to the dentate gyrus. However, neither the role of the CA3-to-DG backpropagation nor its circuit mechanism has been fully understood. Hilar mossy cells receive direct synaptic inputs from CA3 pyramidal cells and make synaptic connections with granule cells in the dentate gyrus. **Methodology:** The synaptic inputs to mossy cells and granule cells in response to SWs were investigated by using whole-cell recordings and extracellular recordings from acute brain slices that spontaneously emit SWs, therefore, mossy cells or granule cells were patch-clamped, while recording the local field potentials from the CA3 stratum pyramidale. **Results:** Results of this study showed that the mossy cells exhibited excitatory synaptic responses to SWs earlier than granule cells. The time lags of EPSPs relative to the SW onsets were 7.3 ± 3.9 msec in mossy cells and 15.7 ± 7.8 msec in granule cells (SDs of 10 and 3 cells, respectively, $p = 0.023$, student's t-test). Furthermore, the ratio of the SW responsive cells was significantly higher in the mossy cells than the granule cells (mossy cell: 10/17 cells, granule cell: 3/15 cells, $p = 0.036$, Fisher's exact test). **Conclusion:** It can be concluded that the synaptic responses of mossy cells to SWs were likely stochastic but more reliable than those of granule cells. Our findings shed light on a novel mechanism underlying the SW backpropagation and provide a new perspective about memory consolidation.

Key words: Sharp wave, ripple, hilar mossy cell, granule cell, backpropagation, patch clamp

Received: October 10, 2016

Accepted: November 08, 2016

Published: December 15, 2016

Citation: Ayako Ouchi, Nobuyoshi Matsumoto and Yuji Ikegaya, 2017. Activation of hilar mossy cells and dentate granule cells during sharp wave/ripples. *Curr. Res. Neurosci.*, 7: 1-8.

Corresponding Author: Yuji Ikegaya, Laboratory of Chemical Pharmacology, Graduate School of Pharmaceutical Sciences, The University of Tokyo, 7-3-1 Hongo, Bunkyo-ku, 113-0033 Tokyo, Japan Tel: +81-3-5841-4780 Fax: +81-3-5841-4786

Copyright: © 2017 Ayako Ouchi *et al.* This is an open access article distributed under the terms of the creative commons attribution License, which permits unrestricted use, distribution and reproduction in any medium, provided the original author and source are credited.

Competing Interest: The authors have declared that no competing interest exists.

Data Availability: All relevant data are within the paper and its supporting information files.

INTRODUCTION

Hippocampal sharp waves (SWs)/ripples spontaneously occur in the hippocampus^{1,2} and are believed to contribute to memory consolidation³ because inhibiting SWs/ripples during post-training rest periods impairs the performance in spatial memory task⁴. The extensive recurrent collateral system of pyramidal cells in the CA3 area plays a role in the initiation of SWs/ripples. The SWs/ripples are then transmitted to the CA1 area through the Schaffer collaterals⁵. However, CA3 pyramidal cells elaborate axonal collaterals in the opposite direction to the Schaffer collaterals and project back to the dentate hilus⁶. The synaptic activity through the backward projection has been evaluated mainly by electrical stimulation and how these synapses are activated during spontaneous activity remains unclear. To address this question, the researchers focused on SWs, which occur spontaneously in the CA3 subregion and backpropagate to the dentate gyrus. This study identified mossy cells in the dentate hilus as candidate cells that mediated the SW backpropagation because these neurons are likely the only type of excitatory neurons that receive direct synaptic inputs from CA3 pyramidal cells. In addition, the axonal fibers of the mossy cells are enriched in the inner one-third of the molecular layer and innervate the proximal dendrites of granule cells⁷⁻⁹. A recent study has demonstrated that mossy cells cannot only excite granule cells but can also indirectly inhibit them by activating nearby GABAergic interneurons¹⁰. Thus, the synaptic inputs to mossy cells and granule cells in response to SWs were investigated by using whole-cell recordings and extracellular recordings from acute brain slices that spontaneously emit SWs¹¹.

MATERIALS AND METHODS

Animal ethics: Animal experiments were performed with the approval of the animal experiments ethics committee at the University of Tokyo (approval No. P24-8) and according to the University of Tokyo guidelines for the care and use of laboratory animals. These experimental protocols were conducted in accordance with the Fundamental Guidelines for the Proper Conduct of Animal Experiments and Related Activities in Academic Research Institutions (Ministry of Education, Culture, Sports, Science and Technology, Notice No. 71 of 2006), the Standards for Breeding and Housing and Pain Alleviation for Experimental Animals (Ministry of the Environment, Notice No. 88 of 2006) and the Guidelines on the Method of Animal Disposal (Prime Minister's Office, Notice No. 40 1995). Whole-cell recordings were made from 25 mice,

out of 48 mice sacrificed. One to three slices per mouse were used in the experiments. All efforts were made to minimize the animals' suffering and the number of animals used.

SW detection: The SWs were detected by thresholding filtered traces on the basis of the signal-to-noise ratio. To detect SWs, LFP traces were band-pass filtered at 2-30 Hz and SW peak times were determined at a threshold at above the mean+5×SD of the baseline noise. The SW onset times were determined at a threshold at above the mean+SD within 50 msec before the SW peak time. The detected events were scrutinized by eye and manually rejected if they were erroneously detected.

Slice preparation: Acute slices were prepared from the medial to ventral part of the hippocampal formation. Postnatal 21-30 day old male ICR mice were deeply anesthetized with isoflurane and decapitated. The brains were rapidly removed and horizontally sliced (400 μm thick) at an angle of 12.7° to the fronto-occipital axis using a vibratome and an ice-cold oxygenated (95% O₂, 5% CO₂) cutting solution consisting of (in mM) 222.1 sucrose, 27 NaHCO₃, 1.4 NaH₂PO₄, 2.5 KCl, 1 CaCl₂, 7 MgSO₄ and 0.5 ascorbic acid. This cutting angle preserved more Schaffer collaterals in the slices¹¹. One to three slices per mouse were used in the experiments. Slices were incubated at 37°C for 30 min and were maintained for at least 1.0 h at room temperature in a submerged chamber filled with oxygenated artificial cerebrospinal fluid (aCSF) containing (in mM) 127 NaCl, 3.5 KCl, 1.24 NaH₂PO₄, 1.3 MgSO₄, 2.4 CaCl₂, 26 NaHCO₃ and 10 d-glucose.

In vitro electrophysiology: Recordings were performed in a submerged chamber perfused at 8 mL min⁻¹ with oxygenated aCSF at 33-35°C. Whole-cell current-clamp recordings were obtained from hilar mossy cells and dentate granule cells in the dentate gyrus visualized with infrared-differential interference contrast microscopy (IR-DIC). Patch pipettes (3-8 MΩ) were filled with a potassium-based solution consisting of (in mM) 135 potassium gluconate, 4 KCl, 10 HEPES, 10 creatine phosphate, 4 Mg-ATP, 0.3 Na₃-GTP, 0.3 EGTA and 0.2% biocytin. Local field potentials (LFPs) were recorded from the CA3 stratum pyramidale using borosilicate glass pipettes (0.6-1 MΩ) filled with aCSF. Once a satisfactory whole-cell recording was obtained, the firing properties of the neuron were identified by applying an 800 msec current from -200 to +200 pA at steps of 50 pA. For each neuron, spike responses to a brief inward current were examined. The data were recorded for 100-300 sec and were used only when the

membrane potential was stabilized (Z-scores of the mean of membrane potentials per 30 sec were between -2 and 2). The signals were digitized at 20 kHz and were filtered with a band of 1-1,000 Hz. The EPSPs were detected at a threshold at above 1 mV, defined as noise level. To define the SW onset-triggered EPSPs, only the single EPSP that had the highest amplitude was selected during a period of ± 100 msec from each SW onset time. The peak latency was determined by computing the peak time from Gaussian-filtered traces and the time lag was calculated from the SW onset time. To analyze the SW participation probability, the 99% confidence interval was estimated in randomly phase-shifted timings of EPSPs for shuffled surrogates from each cell. Data were analyzed offline using custom-made MATLAB routines (Math Works, Natick, MA) and the summarized data were reported as the means \pm standard deviations (SDs) unless otherwise noted. The $p < 0.05$ was considered statistically significant.

Histology: For the visualization of patch-clamped neurons, the slices were fixed in 4% paraformaldehyde and 0.05% glutaraldehyde at 4°C overnight. After the solution was washed out, the sections were incubated with 0.2% Triton X-100, streptavidin-Alexa Fluor 594 conjugate (1:500) and

0.4% NeuroTrace 435/455 Blue Fluorescent Nissl Stain (Thermo Fisher Scientific; N21479) for overnight at 4°C. Fluorescent images were acquired using a confocal microscope (FV1200 Olympus, Tokyo, Japan) and were subsequently merged.

RESULTS

The membrane potentials were recorded from mossy cells or granule cells while the local field potentials were recorded from the CA3 stratum pyramidale (Fig. 1, left). Reconstructed *post hoc* recorded neuron and visualized by a confocal microscope. The morphology of the recorded cells was confirmed using biocytin reconstruction and counterstaining with NeuroTrace Nissl (Fig. 1, right). The SWs occurred spontaneously in all acute slices used. The whole-cell recordings were obtained from a total of 17 mossy cells and 15 granule cells. To ensure the reliability of the electrophysiological experiments, the verification was conducted so that each data passed rejection criteria. Under $I = 0$ conditions, the mean resting potentials of the mossy cells and granule cells were -61.2 ± 4.3 mV and -70.8 ± 4.8 mV, respectively (mean \pm SD of 17 and 15 cells, respectively, $p = 1.53 \times 10^{-6}$, $t_{30} = 5.97$, Student's t-test). The membrane capacitances were 131.3 ± 25.8 pF in mossy cells

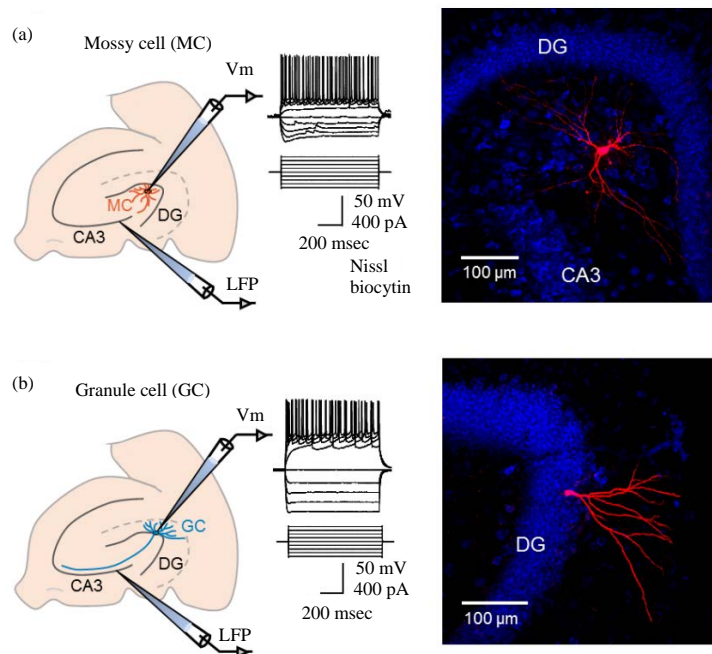


Fig. 1(a-b): Experimental designs. LFPs were recorded from the hippocampal CA3 subregion. (a) Left: A mossy cell (MC) was current-clamp recorded and biocytin was injected through a whole-cell pipette. Right: The recorded neuron was reconstructed *post hoc* and was visualized by a confocal microscope (red). The section was counterstained with NeuroTrace (blue) and (b) Same as MC but for a granule cell (GC)

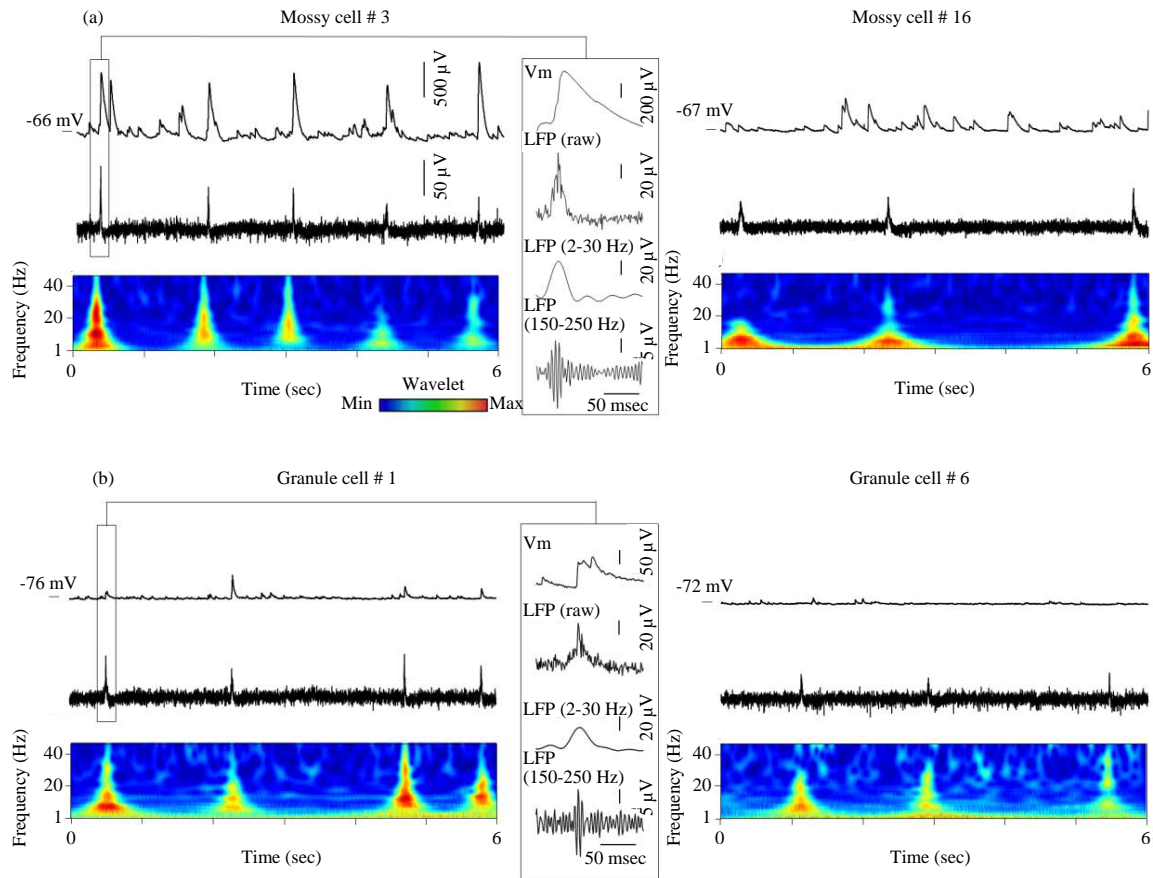


Fig.2(a-b): Mossy and granule cells were divided into responsive and nonresponsive to SW. The representative traces demonstrate membrane potentials (top) and LFPs (middle) of (a) Mossy cells and (b) Granule cells. The wavelet spectrums of LFPs were shown (bottom). Left: Responsive cells, Right: Nonresponsive cells. Each cell number is linked to Fig. 3c. The boxed parts are magnified in the insets, in which the LFP traces are band pass-filtered between 2-30 Hz and 150-250 Hz

and 49.2 ± 18.9 pF in granule cells ($p = 3.25 \times 10^{-11}$, $t_{30} = 10.18$, student's t-test). The membrane resistances were 145.6 ± 39.3 M Ω in mossy cells and 348.0 ± 244.1 M Ω in granule cells ($p = 1.95 \times 10^{-3}$, $t_{30} = 3.40$, Student's t-test). The representative traces of membrane potentials and LFPs are shown in Fig. 2. Occasional source events in LFP traces were a complex of ripples and SWs (Fig. 2a, b, left, inset). In both mossy cells and granule cells, some neurons were depolarized during SWs (Fig. 2a, b, left), whereas others exhibited no obvious responses to SWs (Fig. 2a, b, right).

To define this disparity of the membrane potential responses during SWs, the researchers focused on the response of individual cells. The representative histograms showed the EPSP frequency during the ± 100 msec period relative to the SW onset in both responsive cells (Fig. 3a, b, left) and nonresponsive cells (Fig. 3a, b, right). The SW participation probability was defined as the ratio of the

number of SWs that was accompanied by at least one EPSP to that of the total number of the recorded SWs. The probabilities were compared to that of 10,000 randomly generated surrogates. Among 17 mossy cells and 15 granule cells, 10 and 3 cells, respectively, exhibited the SW participation probabilities that were significantly higher than the 99% confidence interval (Fig. 3c). These cells were defined as responsive cells and were thought to be activated by the CA3-to-DG SW backpropagation. The ratio of the responsive cells was significantly higher in the mossy cells than the granule cells (Fig. 3d, $p = 0.036$, Fisher's exact test). The time lags of EPSPs relative to the SW onsets were 7.3 ± 3.9 msec in mossy cells and were significantly shorter than 15.7 ± 7.8 msec in granule cells (Fig. 3e, SDs of 10 and 3 cells, respectively, $p = 0.023$, $t_{11} = 2.64$, Student's t-test). Therefore, mossy cells participated in the SW backpropagation more frequently than granule cells.

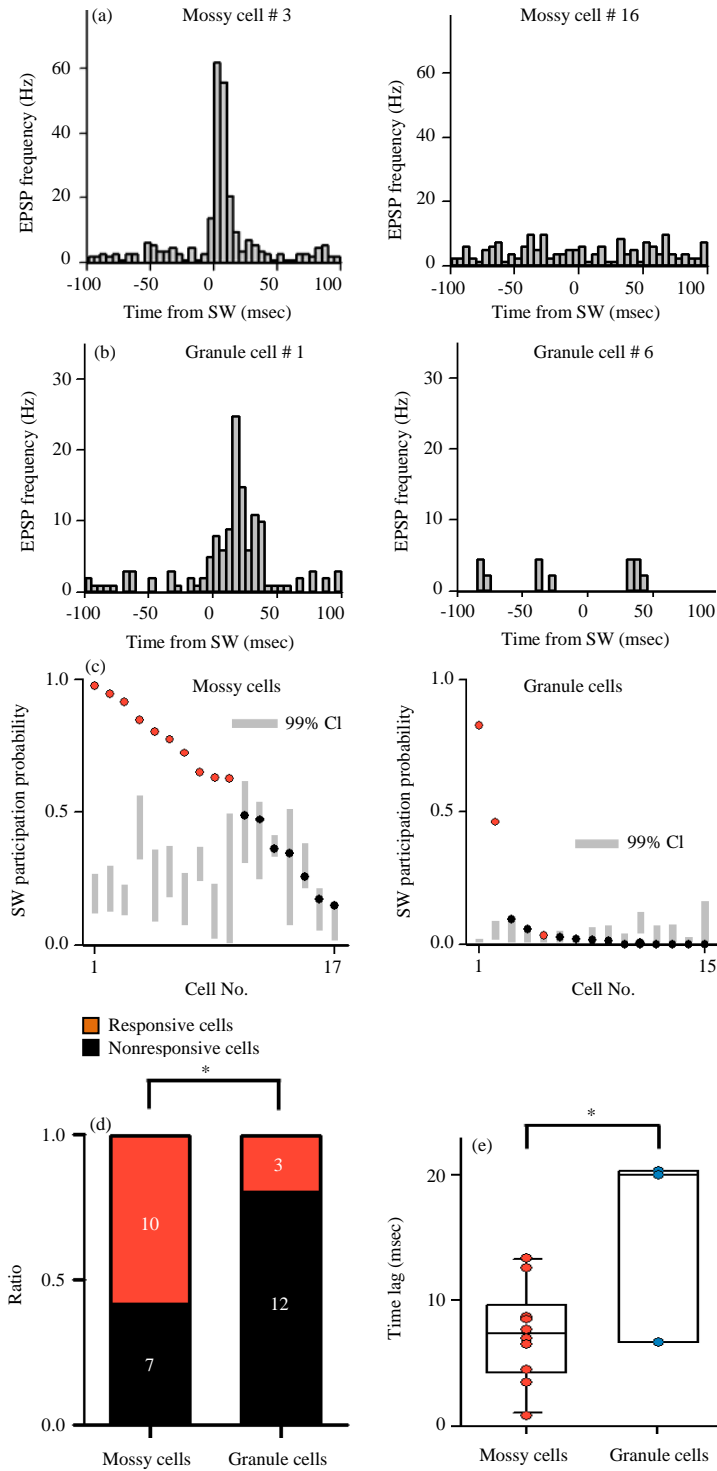


Fig. 3(a-e): Mossy cells participate more frequently in the SW backpropagation. The representative histograms of the EPSP frequencies during ± 100 msec relative to the SW onsets. Responsive (left) and nonresponsive (left) cells of (a) Mossy cells and (b) Granule cells were shown, (c) Mossy cells participated more frequently in SWs than granule cells. Red circles indicate responsive cells. Gray bars indicate the 99% confidence intervals of the corresponding cells, (d) Mossy cells were more responsive to SWs than granule cells. $*p = 0.036$, Fisher's exact test and (e) In responsive cells, the timings of the EPSP onsets relative to the SW onsets were compared between mossy and granule cells. $*p = 0.023$, $t_{11} = 2.64$, Student's t-test, $n = 10$ mossy cells and 3 granule cells

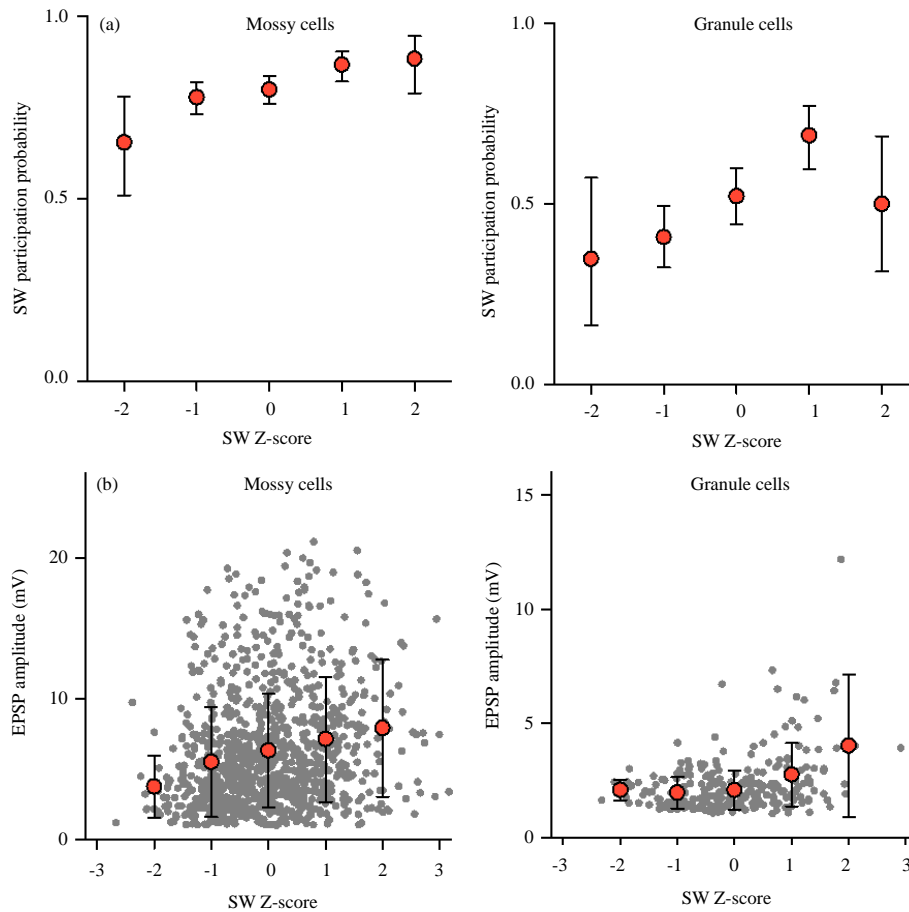


Fig. 4(a-b): SW amplitudes correlate to the EPSP probabilities and the EPSP amplitudes in mossy and granule cells. (a) SW participation probabilities were correlated roughly positively with the SW amplitudes and (b) EPSP amplitudes were correlated positively with the SW amplitudes. Mossy cell: $p = 7.15 \times 10^{-3}$, granule cell: $p = 3.11 \times 10^{-5}$, Jonckheere-Terpstra trend test, $n = 10$ mossy cells and 3 granule cells

The SWs varied in amplitude from event to event (Fig. 2). This variation may reflect the activity levels or the activity patterns in CA3 neurons. The researchers thus focused on individual SW events and examined how the amplitudes of SWs influence on the probabilities of SW-triggered EPSPs in mossy cells and granule cells. Indeed, the EPSP-occurrence probabilities increased with the SW amplitudes (Fig. 4a). Furthermore, when EPSPs occurred in response to SWs, the EPSP amplitudes were also correlated positively with the SWs amplitudes (Fig. 4b, mossy cell: $p = 7.15 \times 10^{-3}$; granule cell: $p = 3.11 \times 10^{-5}$; Jonckheere-Terpstra trend test).

DISCUSSION

The findings in the present study indicated that the mossy cells and granule cells were separated into two groups based on their responses to SWs; some neurons responded with

EPSPs immediately after the generation of CA3 SWs, whereas others exhibited no apparent responses. Mossy cells were more SW-responsive than granule cells and the activation of mossy cells was faster than that of granule cells. Thus, mossy cells are likely to play a more major role in the SW backpropagation.

Previous studies have demonstrated that mossy cells receive large barrages of synaptic inputs induced by fimbria stimulation^{12,13}. Consistent with these studies, spontaneous activity may also efficiently activate mossy cells. Compared to mossy cells, granule cells exhibited more static membrane potentials and were less activated by SWs. This may be merely because mossy cells are activated monosynaptically by CA3 pyramidal cells whereas granule cells are activated disynaptically via mossy cell activity. However, another explanation is possible. Mossy cells are known to modulate excitatory as well as inhibitory synaptic inputs to the dentate

gyrus⁹. Thus, mossy cells activated during SWs may thereafter activate GABAergic interneurons in the hilus and inhibit the SW propagation to the granule cells. Incidentally, CA3c neurons are reported to make collateralization not only in the hilus but also in the granule cell layer and inner molecular layer⁹. Therefore, it is possible that a portion of the granule cells received monosynaptic inputs from CA3 neurons during SWs.

To our knowledge, this study is the first to record the synaptic responses to SWs in mossy cells and granule cells. These cells exhibited diverse responses during SWs. The variability suggests that a few select cells participate in the SW backpropagation. Mossy cells reflect the activity of CA3 SWs more faithfully than granule cells. However, the mechanisms and roles of the CA3-to-DG SW backpropagation are still controversial. In future, simultaneous recording from mossy cells and granule cells will explain a causal relationship between these neurons. *In vitro* patch-clamp recording experiments with pharmacological or optogenetical manipulations will also reveal more detailed contributions of mossy cells in the SW backpropagation.

The previous study has demonstrated that CA1 pyramidal neurons that had been activated while mice had explored a novel environment were preferentially reactivated during SWs in hippocampal slices¹¹. Such specific cell reactivation may also occur in mossy cells, which thereby may contribute to selective memory consolidation. *In vivo* evaluations are required to validate this idea; however, *in vivo* patch-clamp recordings from mossy cells are technically difficult because these cells are spatially sparse in the dentate hilus. Recently, three studies have established methods that can record the activity of mossy cells *in vivo*, using two-photon calcium imaging¹⁴, juxtacellular and extracellular recordings^{15,16}. These techniques will allow us to record spiking activity from individual mossy cells and will reveal the physiological roles of mossy cells in the SW backpropagation.

CONCLUSION

- Mossy cells and granule cells were separated into responsive or non responsive to sharp waves (SWs)
- Mossy cells exhibited excitatory synaptic responses to SWs earlier and more reliable than granule cells in the dentate gyrus
- The findings implicated that mossy cells reflect precisely the activity of SW from CA3

SIGNIFICANT STATEMENT

Sharp waves (SWs)/ripples initiated in the CA3 subregion are transmitted to the CA1 subregion and also back to the dentate gyrus. Although it is known that this backpropagation has a crucial role in memory, the mechanism is not completely understood. The contributions of mossy cells and granule cells to the SW backpropagation were investigated using whole-cell recordings and extracellular recordings. The findings suggest that mossy cells play a major role in relaying SWs backward to the dentate gyrus.

ACKNOWLEDGMENTS

This study was supported by Grants-in-Aid for Science Research A (26250003) and Grants-in-Aid for Science Research on Innovative Areas "Mental Time" (25119004).

REFERENCES

1. Siapas, A.G. and M.A. Wilson, 1998. Coordinated interactions between hippocampal ripples and cortical spindles during slow-wave sleep. *Neuron*, 21: 1123-1128.
2. Buzsaki, G., 1998. Memory consolidation during sleep: A neurophysiological perspective. *J. Sleep Res.*, 7: 17-23.
3. Wilson, M.A. and B.L. McNaughton, 1994. Reactivation of hippocampal ensemble memories during sleep. *Science*, 265: 676-679.
4. Girardeau, G., K. Benchenane, S.I. Wiener, G. Buzsaki and M.B. Zugaro, 2009. Selective suppression of hippocampal ripples impairs spatial memory. *Nat. Neurosci.*, 12: 1222-1223.
5. Csicsvari, J., H. Hirase, A. Mamiya and G. Buzsaki, 2000. Ensemble patterns of hippocampal CA3-CA1 neurons during sharp wave-associated population events. *Neuron*, 28: 585-594.
6. Scharfman, H.E., 2007. The CA3 backprojection to the dentate gyrus. *Progr. Brain Res.*, 163: 627-637.
7. Scharfman, H.E., 1995. Electrophysiological evidence that dentate hilar mossy cells are excitatory and innervate both granule cells and interneurons. *J. Neurophysiol.*, 74: 179-194.
8. Buckmaster, P.S., H.J. Wenzel, D.D. Kunkel and P.A. Schwartzkroin, 1996. Axon arbors and synaptic connections of hippocampal mossy cells in the rat *in vivo*. *J. Compar. Neurol.*, 366: 270-292.
9. Scharfman, H.E. and C.E. Myers, 2012. Hilar mossy cells of the dentate gyrus: A historical perspective. *Frontiers Neural Circ.*, Vol. 6. 10.3389/fncir.2012.00106.
10. Hsu, T.T., C.T. Lee, M.H. Tai and C.C. Lien, 2016. Differential recruitment of dentate gyrus interneuron types by commissural versus perforant pathways. *Cerebral Cortex*, 26: 2715-2727.

11. Mizunuma, M., H. Norimoto, K. Tao, T. Egawa and K. Hanaoka *et al.*, 2014. Unbalanced excitability underlies offline reactivation of behaviorally activated neurons. *Nat. Neurosci.*, 17: 503-505.
12. Scharfman, H.E., 1993. Characteristics of spontaneous and evoked EPSPs recorded from dentate spiny hilar cells in rat hippocampal slices. *J. Neurophysiol.*, 70: 742-757.
13. Strowbridge, B.W., P.S. Buckmaster and P.A. Schwartzkroin, 1992. Potentiation of spontaneous synaptic activity in rat mossy cells. *Neurosci. Lett.*, 142: 205-210.
14. Danielson, N.B., G.F. Turi, M. Ladow, S. Chavlis, P.C. Petrantonakis, P. Poirazi and A. Losonczy, 2017. *In vivo* imaging of dentate gyrus mossy cells in behaving mice. *Neuron*, 93: 552-559.
15. GoodSmith, D., X. Chen, C. Wang, S.H. Kim and H. Song *et al.*, 2017. Spatial representations of granule cells and mossy cells of the dentate gyrus. *Neuron*, 93: 677-690.
16. Senzai, Y. and G. Buzsaki, 2017. Physiological properties and behavioral correlates of hippocampal granule cells and mossy cells. *Neuron*, 93: 691-704.